

Article

Channel Allocation in Wireless Networks with Directional Antennas

Hong-Ning Dai ^{1,*}, Kam-Wing Ng ² and Min-You Wu ³

¹ Faculty of Information Technology, Macau University of Science and Technology, Macau

² Department of Computer Science and Engineering, The Chinese University of Hong Kong, Hong Kong; E-Mail: kwng@cse.cuhk.edu.hk

³ Department of Computer Science and Engineering, Shanghai Jiao Tong University, Shanghai 200030, China; E-Mail: wu-my@cs.sjtu.edu.cn

* Author to whom correspondence should be addressed; E-Mail: hndai@ieee.org;
Tel.: +853-8897-2154; Fax:+853-2882-3280.

Received: 1 March 2013; in revised form: 29 March 2013 / Accepted: 2 April 2013 /

Published: 16 April 2013

Abstract: In this paper, we study the channel allocation in multi-channel wireless *ad hoc* networks with directional antennas. In particular, we investigate the problem: given a set of wireless nodes equipped with directional antennas, how many channels are needed to ensure collision-free communications? We derive the upper bounds on the number of channels, which heavily depend on the node density and the interference ratio (*i.e.*, the ratio of the interference range to the transmission range). We construct several scenarios to examine the tightness of the derived bounds. We also take the side-lobes and back-lobes as well as the signal path loss into our analysis. Our results can be used to estimate the number of channels required for a practical wireless network (e.g., wireless sensor network) with directional antennas.

Keywords: multiple channels; channel allocation; wireless *ad hoc* networks; wireless sensor networks; directional antennas; graph theory

1. Introduction

With the proliferation of various wireless devices and wireless communication services, the demand for wireless spectrum is constantly increasing and the available wireless spectrum becomes scarce. Therefore, the study on the effective and sufficient channel allocation schemes of the wireless spectrum has received extensive attention from both academia and industry. However, most of the current studies on the channel allocation schemes are focused on wireless *ad hoc* networks with *omni-directional antennas (OMN)*, which radiate wireless signals in all directions and consequently lead to high interference to other concurrent transmissions. As a result, an omni-directional antenna has low spectrum reuse. We call such wireless *ad hoc* networks with omni-directional antennas as *OMN* networks. Most of the current wireless sensor networks (*WSNs*) are *OMN* networks.

Compared with an omni-directional antenna, a *directional antenna (DIR)* can concentrate wireless signals on the desired direction and lead to low interference to other current transmissions. Potentially, a directional antenna can improve the spectrum reuse and consequently improve the network performance. Specifically, it is shown in [1,2] that using directional antennas in *WSNs* can significantly improve the network capacity and reduce the end-to-end delay. We name such wireless networks with directional antennas as *DIR* networks. In this paper, we study the channel allocation of *DIR* networks. In the following, we first survey the related work and then summarize our research contributions.

1.1. Related Work

Many recent studies focused on using multiple channels in *OMN* networks to improve the network performance. In particular, the experimental results of [3–8] show that using multiple channels can significantly improve the network throughput. One possible reason is that using multiple channels can separate multiple concurrent transmissions in frequency domain. On the other hand, the relationship between the number of channels and the network capacity were studied in [9,10]. More specifically, it is shown in [9] that the capacity of *OMN* networks has different bounds, which only depend on the ratio of the number of interfaces to the number of channels. Reference [10] studied the problem by using *linear programming*. More specifically, the *interference constraint* and *flow constraint* were defined in [10]. In addition, the link scheduling and channel allocation problem has been studied in [11]. Specifically, in [11], a *conflict graph* was proposed to model the constraints, and the channel assignment problem was converted into a graph coloring problem. Furthermore, the general channel allocation problem in *OMN* networks was studied in [12]. Moreover, [13] first applied stochastic optimization in channel allocation in *OMN* networks.

However, most of the current studies on the channel allocation are focused on *OMN* networks. Recent studies such as [14–21] found that applying *directional antennas* instead of omni-directional antennas in wireless networks can greatly improve the network capacity. For example, the analytical results in [14] show that using directional antenna in arbitrary networks achieves a capacity gain of $2\pi/\sqrt{\alpha\beta}$ when both transmission and reception are directional, where α and β are transmitter and receiver antenna beamwidths, respectively. Under random networks, the capacity gain is $4\pi^2/(\alpha\beta)$. However, these studies only considered the single channel in *DIR* networks. There are few studies on the multi-channel allocation of *DIR* networks, which are shown to have higher performance than

OMN networks [14,20,22]. In particular, the channel allocation in IEEE 802.11-based mesh networks with directional antennas was studied in [23]. However, the allocation scheme of this study can only apply for the specific network, in which a wireless station (or a node) can simultaneously transmit to a number of other stations, or simultaneously receive from a number of other stations, but a station cannot simultaneously transmit and receive (*i.e.*, the half-duplexity is still in place).

1.2. Contributions

The primary research contributions of our paper can be summarized as follows.

- We study the channel allocation in general *DIR* networks. In particular, we try to answer the question: how many channels are needed to ensure collision-free communications in a *DIR* network.
- We formulate the channel allocation problem as a *graph coloring* problem. We derive the upper bounds on the number of channels to ensure collision-free communications in a *DIR* network. It is shown that the upper bounds on the number of channels heavily depend on the node density and the interference ratio.
- We compare our derived upper bounds with the results derived from *OMN* networks. We also investigate the tightness of our derived upper bounds by constructing several scenarios.
- We also take the side-lobes and back-lobes of a directional antenna as well as the physical channel characteristics (e.g., the signal path loss) into account. Specifically, our results show that when the beamwidth of a directional antenna is quite narrow, the effect of the side-lobes and back-lobes is so small that they can often be ignored.
- Our results are also useful in practice. In particular, our results can be used to roughly estimate the number of channels needed in the given configuration of a wireless network (e.g., a *WSN* with directional antennas). On the other hand, when the number of available channels is limited, our results can be used to suggest the proper network setting.

The remainder of the paper is organized as follows. In Section 2, we describe the models and give the problem formulation. Section 3 presents the derived upper bounds on the number of channels under different values of the interference ratio. In Section 4, we construct several communication scenarios and examine the tightness of our derived bounds. Section 5 compares our results with those derived with omni-directional antennas and presents some useful implications. Finally, we conclude our work in Section 7.

2. Models and Problem Formulation

In order to clarify our analysis, we firstly propose a directional antenna model and an interference model in Section 2.1. Then Section 2.2 gives the definitions for a link set, a valid assignment as well as the node density, and presents the problem formation for the upper bound on the number of channels. In Section 2.3, we define the conflict graph.

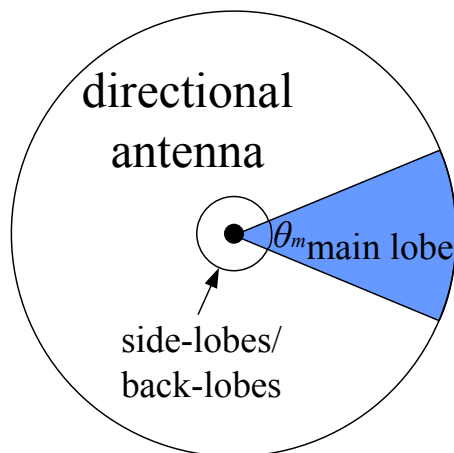
2.1. Models

2.1.1. Antenna Model

The radiation pattern of a directional antenna is often depicted as the gain values in each direction in space. We can project the radiation pattern of an antenna to an azimuthal or elevation plane. The projection of the pattern typically has a main lobe (beam) of the peak gain and side-lobes and back-lobes of smaller gains.

Since modeling a real antenna with precise values for main and side-/back-lobes is difficult, we use an approximate antenna pattern in [15]. In an azimuthal plane, the main lobe of antenna can be depicted as a sector with angle θ_m , which is denoted as the beamwidth of the antenna. The side-lobes and back-lobes are aggregated to a circle, as shown in Figure 1. The narrower the main beamwidth of the antenna is, the smaller the side-lobes and back-lobes are. Let us take the above antenna model as an example: the gain of the main beam is more than 100 times of the gain of side-lobes when the main beamwidth is less than 40° [15]. Thus, we temporarily ignore the effects of the side-lobe and back-lobes of an antenna in the follow sections. Specifically, we will extend our analysis with the side-lobes and back-lobes in Section 6.

Figure 1. The Antenna Model.



Our simplified model assumes that the directional antenna gain is within the main beam. The gain outside the main beam is assumed to be zero. At any time, the antenna beam can only be pointed to a certain direction, as shown in Figure 1, in which the antenna is pointing to the right.

2.1.2. Interference Model

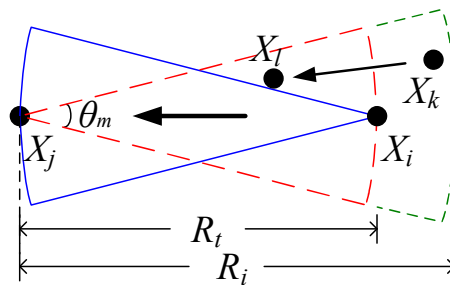
We propose an interference model, which extends the *Protocol Model* in [24] to directional antennas. Our model only considers directional transmission and directional reception, which can maximize the benefits of directional antennas.

Two nodes X_i and X_j can establish a bi-directional link denoted by l_{ij} if and only if the following conditions are satisfied.

- (1) X_j is within the *transmission range* of X_i and X_i is within the *transmission range* of X_j .
- (2) X_j is covered by the antenna beam of X_i . Similarly, X_i is also covered by the antenna beam of X_j .
- (3) No other node within the *interference range*(the interference range is used to denote the maximum distance within which a node can be interfered by an interfering signal) is simultaneously transmitting over the same channel and in the same direction toward X_j .

We call two nodes in *conflict* with each other if they are located within the interference range of each other and their antenna beams are pointed toward each other. For example, in Figure 2, node X_k within the interference range of node X_j may conflict with X_j . Link l_{ij} *conflicts* with link l_{kl} if either node of one link conflicts with either node of the other link.

Figure 2. The Interference Model.



2.2. Definitions and Problem Formulation

In this paper, we assume that there are n nodes in a plane and each node has only one antenna (interface), *i.e.*, it can only transmit or receive with at most one neighboring node at one time.

We also assume that each node is equipped with an identical antenna with the same beamwidth θ_m . Each node also has the same *transmission range*, denoted by R_t and the same *interference range*, denoted by R_i . Typically, R_i is no less than R_t , *i.e.*, $R_i \geq R_t$.

Basic definitions are stated as follows.

Definition 1 Link Set. A link set is defined as a set of links among which no two links in this set share common nodes. Such a link set is denoted as LS . A link set is used to describe a set of links that need to act simultaneously.

Definition 2 Valid Assignment. A valid assignment to a link set is an assignment of channels such that no two conflicting links are assigned an identical channel. A link set is called a Schedulable Link Set if and only if there exists a valid assignment for the link set.

Definition 3 Interference Ratio. The interference ratio is the ratio of the interference range to the transmission range, *i.e.*, $r = R_i/R_t$. Since $R_i \geq R_t$, it is obvious that the interference ratio $r \geq 1$. The number of interfering nodes around a node heavily depends on the interference ratio.

Definition 4 Node Density. There are n nodes randomly located in the plane. Let S denote the (infinite) set of sectors on the plane with radius R_i and angle θ_m . The number of nodes within sector s is denoted as $N(s)$. The density of nodes is defined as $D = \max_{s \in S} N(s)$.

In order to compare our derived results to those with *OMN* networks [12], we re-state the definition here.

Definition 5 [12] Node Density with Omni-directional Antennas. *There are n nodes uniformly located in the plane. Let C denote the (infinite) set of circles on the plane with radius R_i . The number of nodes within circle c is denoted as $N(c)$. The density of nodes is defined as $D_o = \max_{c \in C} N(c)$.*

Then we give the definition of the upper bound on the number of channels to ensure collision-free communications in *DIR* networks.

Definition 6 Upper Bound on the number of channels. *There exist possibly many valid link sets, which represent different combination of communication pairs among the nodes. The problem is to find a number, denoted as U , such that any link set LS derived from n nodes is schedulable using U channels. In other word, U is the upper bound of channels needed to ensure a collision-free link assignment.*

2.3. Conflict Graph

The link assignment problem can be converted to a *conflict graph* problem, which is first addressed in [11]. A conflict graph is used to model the effects of interference.

Definition 7 Conflict Graph. *We define a graph in which every link from a link set LS can be represented by a vertex. Two vertices in the graph are connected by an edge if and only if the two links conflict. Such a graph is called a conflict graph. The conflict graph G constructed from link set LS is denoted as $G(LS)$.*

3. Upper Bounds on the Number of Channels

In this section, we first convert the channel assignment problem of *DIR* networks to the vertex coloring problem in graph theory. We then derive the upper bounds on the number of channels.

3.1. Background Results

By constructing the conflict graph for a link set, and representing each channel by a different color, we found that the requirement that no two conflicting links share the same channel is equivalent to the constraint that no two adjacent vertices share the same color in graph coloring. Therefore, the problem of channel assignment on a link set can be converted to the classical vertex coloring problem (in graph theory, the vertex coloring problem is a way of assigning “labels”—colors—to vertices of a graph such that no two adjacent vertices share the same color) on the conflict graph. The vertex coloring problem, as one of the most fundamental problems in graph theory, is known to be NP-hard even in the very restricted classes of planar graphs [25]. A coloring is regarded as valid if no two adjacent vertices use the same color.

The minimum number for a valid coloring of vertices in a graph G is denoted by a *chromatic* number, $\chi(G)$. There are two well-known results on the upper bound of $\chi(G)$, which will be used to derive our results.

Lemma 1 [26] If $\Delta(G)$ denotes the largest degree among G 's vertices, i.e., $\Delta(G) = \max_{v \in G} \text{Degree}(v)$, then we have

$$\chi(G) \leq \Delta(G) + 1$$

Lemma 2 [27] If G contains a subgraph H in which each node has a degree at least $d > 0$, we define such degree as $LD(H) = \min_{v \in H} \text{Degree}(v)$. We have

$$\chi(G) \leq \delta(G) + 1$$

where the maximum degree among all the $LD(H)$ is denoted by $\delta(G) = \max_{H \subseteq G} LD(H)$.

3.2. Upper Bounds on the Number of Channels

We then derive several upper bounds under different network settings in terms of the interference ratio r .

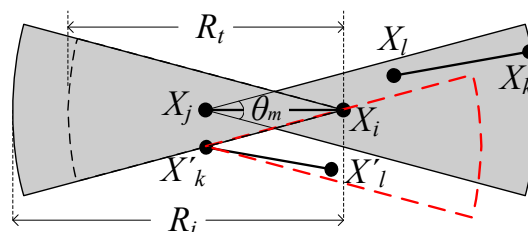
Theorem 1 If there are n nodes in a planar area with the density D and each node is equipped with an antenna with the identical beamwidth θ_m , for any valid link set LS derived from the n nodes, the corresponding conflict graph $G(LS)$ can be colored by using $2D - 1$ colors.

Proof. Consider link l_{ij} that consists of nodes X_i and X_j , as shown in Figure 3. The interference region is denoted as two sectors with radius R_i and angle θ_m (the gray area in Figure 3). From the definition of node density, each sector has at most D nodes. Other than nodes X_i and X_j , there are at most $D - 1$ nodes in either sector. After we combine the nodes in the two sectors, the gray area contains no more than $2D - 2$ nodes excluding nodes X_i and X_j .

Suppose link l_{kl} is one of the links that conflicts with l_{ij} . It is obvious that at least one node of that link, e.g., X_k , should be in X_j 's interference region, the gray sector centered at X_j in Figure 3. At the same time, the antenna of X_k should be pointed to X_j if it can interfere with X_j . Thus, X_k 's interference region must also cover X_j . So, $|X_k - X_j| \leq R_i$. Since the antenna beam of the other node X_l should be turned toward X_k , it must also fall in the interference region of X_j , as shown in Figure 3. Hence, $|X_l - X_j| \leq R_i$.

It seems that any link that conflicts with link l_{ij} must fall in the gray area representing the interference regions of nodes X_i and X_j . However, consider the case that X'_k and X'_l form a link l'_{kl} in Figure 3. X'_l is outside the gray region of l_{ij} , but X'_k can interfere with X_i since its beam covers X_i . So, a link conflicting with link l_{ij} must contain at least one node falling in the gray area.

Figure 3. The Interference Region.



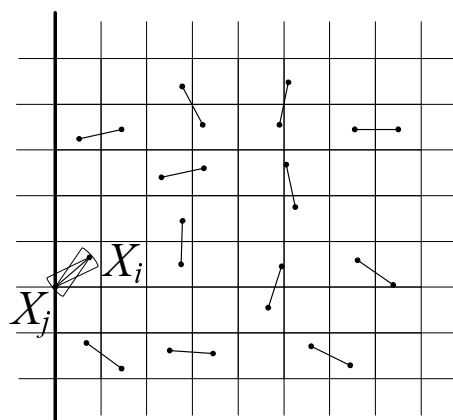
Therefore, there are at most $2D - 2$ links that conflict with l_{ij} . Hence, the maximum degree of the vertices of G is $\Delta(G) \leq 2D - 2$. From Lemma 1, the conflict graph can be colored by using $2D - 1$ colors. □

Theorem 1 can be applied to any settings of the interference ratio r . When r is greater than 1, we can get tighter upper bounds. Specifically, we have the result when $r = 2$.

Theorem 2 *When $r = 2$ and n nodes are distributed in a planar area with density D , and each node is equipped with an antenna with the identical beamwidth θ_m , for any valid link set LS derived from those n nodes, the corresponding conflict graph $G(LS)$ can be colored by using $\frac{3}{2}D$ colors.*

Proof. Without loss of generality, we assume $R_t = 1$ so $R_i = 2$. Since the number of nodes n is a finite number, the number of links derived from n is also a finite number. Given a finite number of links on the plane, we can always find a line, such that at least one node is on the line, and all the other nodes are on the right hand side of the plane (as shown in Figure 4). We denote the node on the line as X_j , and the other node on the corresponding link l_{ij} is X_i . Then we will calculate the number of links that may conflict with link l_{ij} .

Figure 4. The plane is divided into two parts.

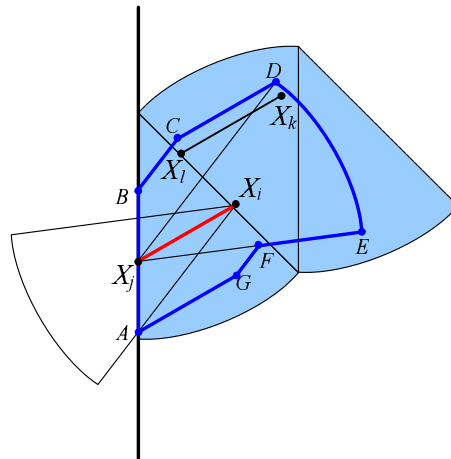


Let us consider link l_{ij} consisting of two nodes X_i and X_j (as shown in Figure 5). For any link l_{kl} that interferes with node X_j , at least one node of that link must fall in the interference range of X_j . Thus, any interfering link must have an acute angle with link l_{ij} . Therefore, we draw a line in parallel with the line segment X_iX_j and a line in parallel with the upper border of the interference region of X_j to bound those interfering nodes. Similarly, we draw other two lines in parallel with X_iX_j and the lower border of the interference region of X_i . Those lines and the arc of the interference region of X_j form the region $ABCDEFG$ with the bold border, as shown in Figure 5 (note that the length of CD is equal to the length of AG , which is equal to the length of X_kX_l). Thus, those interfering nodes should all fall in this region.

Then we illustrate that this region can be covered by three identical sectors with radius $R_i = 2$ and angle θ_m . We place these three sectors as follows. First, we put a sector with one of its edge tightly clinging to the thick line as shown in Figure 5. By calculating the coordinates of point A and point B , we can prove that R_i is greater than segment AB . Then we place the second sector next to the first one as shown in Figure 5. Similarly, we can prove that points C and D fall in the second sector by calculating

the coordinates of C and D . Then we put the third sector next to the second one. Point E falls in the third sector. Points F and G also fall in the first sector. So, the region $ABCDEFG$ can be covered by the three sectors.

Figure 5. The proof of Theorem 2.



Since the region $ABCDEFG$ can be covered by three identical sectors with radius R_i and angle θ_m , by definition of the node density, the number of nodes in region $ABCDEFG$ is at most $3D$. Those $3D$ nodes can form at most $\frac{3}{2}D$ links in this area. Other than link l_{ij} , there are at most $\frac{3}{2}D - 1$ links that can interfere with link l_{ij} . Therefore, every vertex in subgraph H (the gray area in Figure 5) of G has a vertex with degree at most $\frac{3}{2}D - 1$. From Lemma 2, the conflict graph can be colored by using $\frac{3}{2}D$ colors. \square

Note that the result of Theorem 2 also holds for any $r > 2$. More specifically, we have the following result.

Theorem 3 *If an upper bound U is valid for the interference ratio $r = r_1$, $r_1 \geq 2$ and $r_2 > r_1$, then the upper bound U is also valid for $r = r_2$.*

Proof. Without loss of generality, we have the assumption that the interference range is fixed at $R_i = 1$ in both following two cases.

Case I ($r = r_1$):

The transmission range in this case $R_{t1} = \frac{R_i}{r_1} = \frac{1}{r_1}$ and U is a valid upper bound.

Case II ($r = r_2$):

Thus, the transmission range in the second case $R_{t2} = \frac{R_i}{r_2} = \frac{1}{r_2}$. Since $r_2 > r_1$, we have $R_{t1} > R_{t2}$. This means that the transmission range R_{t1} in the first case ($r = r_1$) is larger than the transmission range R_{t2} in the second case ($r = r_2$). That is to say *any valid link set LS in the second case is also valid in the first case*. Since interference ranges are equal in the two cases, link set LS will result in the same conflict graph in the two cases. Recall the assumption that when $r = r_1$, U colors are enough to satisfy $G(LS)$. Therefore, U is also a valid upper bound when $r = r_2$. \square

As shown in Theorem 3, the upper bound is monotonically non-increasing as interference ratio r increases. Intuitively, the larger the interference ratio r is, the further reduced the upper bound U can be. When $r = 4$, we have the following result.

Theorem 4 When $r = 4$ and n nodes are distributed in a planar area with density D , and each node is equipped with an antenna with beamwidth θ_m , for any valid link set LS derived from those n nodes, the corresponding conflict graph $G(LS)$ can be colored by using D colors.

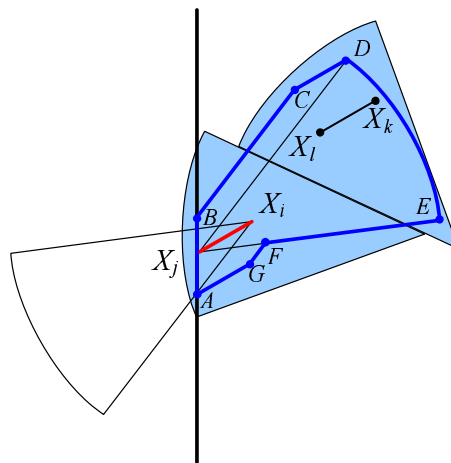
Proof. We take the similar proof techniques to prove Theorem 4. Without loss of generality, we assume that $R_t = 1$ and $R_i = 4$.

From Lemma 2, it is sufficient to prove that $\delta(G) \leq D - 1$. This is equivalent to prove that every vertex of every subgraph of G has a degree at most $D - 1$. In other words, we prove that for every subset of link set LS , there exists link l_{ij} such that there are at most $D - 1$ links that interfere with link l_{ij} .

Similar to the proof of Theorem 2, we also show that the nodes interfering link l_{ij} will all fall in a region that can be covered by two identical sectors with radius R_i and angle θ_m .

As shown in Figure 6, for any link l_{kl} that interferes with node X_j , at least one node of that link must fall in the interference range of X_j . The other node of such link l_{kl} must fall into region $ABCDEFGG$ with the bold border.

Figure 6. The proof of Theorem 4.



We illustrate that this region with the bold border can be covered by two identical sectors with radius $R_i = 2$ and angle θ_m . We place these two sectors as follows. First, we put a sector horizontally. By calculating the coordinates of point A and point B , we can prove that points A and B are falling into the first sector. Then we put the second sector contiguous to the first sector. By calculating the coordinates of points C , D and E , we can prove that points C , D and E fall into the second sector. Similarly, we can prove that points F and G fall into the first sector. So, the region $ABCDEFGG$ can be covered by the two sectors.

Since the region $ABCDEFGG$ can be covered by two identical sectors with radius R_i and angle θ_m , by definition of the node density, the number of nodes in region $ABCDEFGG$ is at most $2D$. Those $2D$ nodes can form at most D links in this area. Other than link l_{ij} , there are at most $D - 1$ links that can interfere with link l_{ij} . Therefore, every vertex in subgraph H (the gray area in Figure 6) of G has a vertex with degree at most $D - 1$. From Lemma 2, the conflict graph can be colored by using D colors. \square

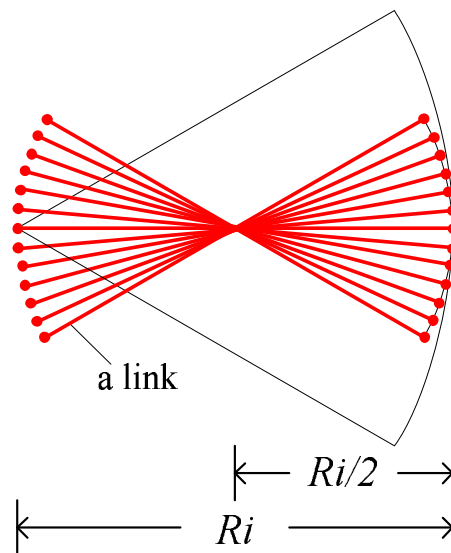
4. Tightness of the Upper Bounds

In this section, we construct several scenarios to examine the tightness of the derived upper bounds. In particular, we have the following results.

Theorem 5 When $r = 1$, the upper bound cannot be reduced to be lower than $D - 1$.

Proof. When $r = 1$, $R_i = R_t$. We construct a scenario, as shown in Figure 7. The density D is 14 in Figure 7. We first draw a sector of radius $R_i/2$ and angle θ_m . Then we place $D - 1$ (13) nodes equally on the arc of the sector with radius $R_i/2$. For each node on the circle, we establish a link with length $R_t = R_i$ toward the center of the sector, as shown in Figure 7.

Figure 7. The proof of Theorem 5.



It is obvious that the node set we have just constructed is of density D since there are D nodes within the sector of radius R_i and angle θ_m . For the link set from the constructed node set, the corresponding conflict graph is a $(D - 1)$ -clique (*i.e.*, each link interferes with each other), which needs exactly $D - 1$ colors to color. So the upper bound cannot be lower than $D - 1$. \square

When the interference ratio r is increased, the upper bound can also be reduced. More specifically, when $r \geq 2$, we have the following result.

Theorem 6 When $r \geq 2$, the upper bound cannot be reduced to lower than $\lfloor \frac{\beta}{\theta_m} \cdot \frac{D}{2} \rfloor + 1$, where $\beta = 2 \arctan\left(\frac{\tan \frac{\theta_m}{2} \cdot (\sqrt{(2r-1) \tan^2 \frac{\theta_m}{2} + r^2} - (r-1))}{(r-1) \tan^2 \frac{\theta_m}{2} + \sqrt{(2r-1) \tan^2 \frac{\theta_m}{2} + r^2}}\right)$, which only depends on the beamwidth θ_m and the interference ratio r .

Proof. When $r \geq 2$, we construct a scenario shown in Figure 8. We first draw a sector with radius $d \geq R_i/2$ and put n nodes equally on the arc of the sector. For each node on the circle, we establish a link with length R_t directed against the center of the sector, as shown in Figure 8.

For this example, the node density $D = 2n$ since we can put a sector with radius R_i and angle θ_m to cover those n links (each link has two nodes). Then, we need to calculate the number of links that a

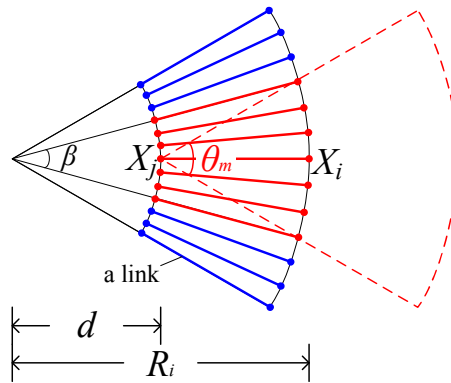
link can interfere with. We take link l_{ij} as an example. All the nodes falling in the interference region of nodes X_j may interfere with node X_i . In order to calculate the number of susceptible links, we need to calculate the *coverage angle*, denoted as β . The details on the calculation of the coverage angle β can be found in Appendix A. Thus, we have

$$\beta = 2 \arctan\left(\frac{\tan \frac{\theta_m}{2} \cdot (\sqrt{(R_i^2 - d^2) \tan^2 \frac{\theta_m}{2} + R_i^2} - d)}{d \tan^2 \frac{\theta_m}{2} + \sqrt{(R_i^2 - d^2) \tan^2 \frac{\theta_m}{2} + R_i^2}}\right) \tag{1}$$

Since $R_i = r \cdot R_t$ and $d = R_i - R_t = (r - 1)R_t$, we substitute the corresponding parts in Equation (1). Then we have

$$\beta = 2 \arctan\left(\frac{\tan \frac{\theta_m}{2} \cdot (\sqrt{(2r - 1) \tan^2 \frac{\theta_m}{2} + r^2} - (r - 1))}{(r - 1) \tan^2 \frac{\theta_m}{2} + \sqrt{(2r - 1) \tan^2 \frac{\theta_m}{2} + r^2}}\right) \tag{2}$$

Figure 8. The proof of Theorem 6.



From Equation (2), the coverage angle β is less than the beamwidth θ_m . It only depends on θ_m and the interference ratio r . This angle monotonously increases with θ_m when $0 < \theta_m \leq \frac{\pi}{2}$. Furthermore, it monotonously decreases with the increased interference ratio r . There are nearly $\lfloor \frac{\beta}{\theta_m} \cdot \frac{D}{2} \rfloor + 1$ links falling in the interference region of node X_j . Thus, in order to separate those links, we need at least $\lfloor \frac{\beta}{\theta_m} \cdot \frac{D}{2} \rfloor + 1$ colors. □

It is shown in Theorem 6 that the number of required channels can be reduced when r is increased.

Theorem 7 *The upper bound cannot be reduced to lower than $\frac{1}{2}D$, for any r and any θ_m .*

Proof. Suppose that there are D nodes that are closely located. The distance between any two of them is ϵ , where ϵ is a quite small number and $\epsilon > 0$. Any link is constructed from any two of the D nodes. When the distance is quite narrow, the collisions among links are quite high and any link can almost conflict with other links. So, there are $\frac{1}{2}D$ links that conflict with each other. Therefore, the number of channels cannot be reduced to $D/2$. □

5. Discussions and Implications

We summarize our results in Table 1. We also compare our results with omni-directional cases [12]. Note that we assume $R_i = 1$ is fixed and R_t is adjustable. The coverage angle β is given in Equation (1), which decreases with the increased interference ratio r . When $r = 2$, the angle is denoted by β_1 . When $r = 4$, the angle is denoted by β_2 . Thus, we have $\beta_2 < \beta_1$.

Table 1. Comparisons of *OMN* networks and *DIR* networks.

r	<i>OMN</i> Networks [12]		<i>DIR</i> Networks	
	Upper bounds	Lower constraints	Upper bounds	Lower constraints
1	$2D_o - 3$	$D_o - 1$	$2D - 1$	$D - 1$
2	$\frac{3}{2}D_o$	$\frac{2}{3}(D_o - 1)$	$\frac{3}{2}D$	$\lfloor \frac{\beta_1}{\theta_m} \frac{D}{2} \rfloor + 1$
4	D_o	$\frac{1}{2}D_o$	D	$\lfloor \frac{\beta_2}{\theta_m} \frac{D}{2} \rfloor + 1$
∞	$\frac{1}{2}D_o$	$\frac{1}{2}D_o$	$\frac{1}{2}D$	1

When interference ratio $r = 1$, the upper bound for the network with directional antennas is $2D - 1$ and the upper bound for the network with omni-directional antennas is $2D_o - 3$. Different from the node density D with directional antennas, D_o is defined as the maximum number of nodes within a circle of interference range. Generally, we have $D \neq D_o$.

When $r = 2$, the upper bound on the number of channels is $\frac{3}{2}D$ for directional antennas and $\frac{3}{2}D_o$ for omni-directional antennas. Similarly, when $r = 4$, the upper bound is reduced to D for directional antennas and D_o for omni-directional antennas. From those results, we have found that the number of channels needed for a collision-free transmission scales linearly with the node density D , and is non-increasing as the interference ratio r increases.

When the interference ratio r approximates the infinity, then R_t approximates 0. This means all links have length 0. So, any link will conflict with at most $\frac{1}{2}D - 1$ links in the directional case and $\frac{1}{2}D_o - 1$ links in the omni-directional case.

From Table 1, we also observe that upper bounds derived from the omni-directional antennas have almost the same coefficients as those derived from the directional antennas except for the case when $r = 1$ (although they have different node densities, *i.e.*, D and D_o). Both the upper bounds derived from the omni-directional case and those derived from the directional case heavily depend on the node density and the interference ratio. An interesting question is whether the upper bounds are independent of the actual radiation patterns of antennas.

Our derived theoretical results can be applied to solve many practical problems. For example, given a wireless network with a number of wireless nodes, our derived bounds can be used to estimate the number of channels required to ensure a collision-free communication. For another example, when the number of channels is given (e.g., there are 14 channels but only three orthogonal channels available in IEEE 802.11), our results can be used to offer suggestions on the node density in the node deployment or suggestions on the channel assignment for a given network.

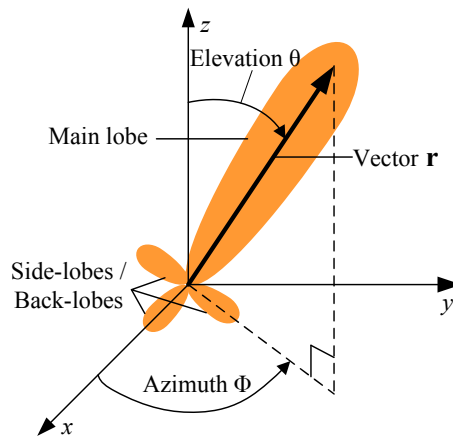
6. Extension with Side-Lobes/Back-Lobes as Well as the Path Loss Effect

In this section, we take side-lobes and back-lobes of a directional antenna as well as the signal path loss effect into our analysis. We next derive the results on the upper bounds of the number of channels with consideration of the above factors.

6.1. Antenna Model with Side-Lobes and Back-Lobes

To measure the *directivity* of an antenna, we often consider the three-dimensional spatial distribution of *antenna gains*, which is called the *radiation pattern* of an antenna. Figure 9 shows the radiation pattern of a realistic directional antenna in 3-D space, which typically consists of the *main lobe* (or *beam*) with the largest *radiation intensity* and the *side-lobes* and *back-lobes* with smaller radiation intensity.

Figure 9. Radiation pattern of a realistic directional antenna.



As shown in Figure 9, we use vector \mathbf{r} to represent the direction of the radiation intensity in 3-D space. In particular, we use θ to represent the angle between the vector \mathbf{r} and the z -axis ($\theta \in (0, \pi)$), and ϕ to represent the angle between the x -axis and the projection of the vector \mathbf{r} into the xy plane ($\phi \in (0, 2\pi)$). We then define the gain of an antenna as

$$G(\theta, \phi) = \eta \frac{U(\theta, \phi)}{U_o} \tag{3}$$

where η is the efficiency factor, which is usually set to be 1 since all the antennas in this paper are assumed to be lossless, $U(\theta, \phi)$ is the *radiation intensity*, which is defined as the power radiated from an antenna per unit solid angle, and U_o denotes radiation intensity of an *isotropic* antenna with the same radiation power P_{rad} as a directional antenna. Note that an *isotropic* antenna is a point that radiates/collects radio power uniformly in all directions in 3-D space. In this paper, we regard an isotropic antenna as being equivalent to an omni-directional antenna since both of them have the same projected *radiation pattern*—a circular area in a 2-D plane.

We next analyze the antenna gain of omni-directional antennas and the antenna gain of directional antennas, which will be used in the physical channel model in Section 6.2.

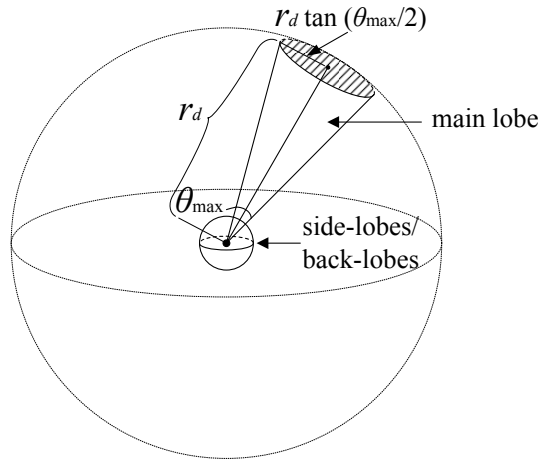
6.1.1. Omni-Directional Antenna

It is obvious that an omni-directional antenna has antenna gain $G_o = 1$ since an omni-directional antenna radiates the power uniformly in all directions, *i.e.*, $U(\theta, \phi) = U_o$. Note that we consider the linear gain instead of logarithmic gain (dBi) for an antenna in this paper in order to maintain consistency with the physical channel model (see Section 6.2).

6.1.2. Directional Antenna

As mentioned in Section 2, we consider an approximated radiation pattern of directional antennas [15]. In this model, the main lobe of a directional antenna is represented as a cone with angle θ_m and side-lobes and back-lobes are approximated as a sphere with beamwidth $2\pi - \theta_m$. Figure 10 shows the approximated radiation pattern of a directional antenna.

Figure 10. Approximated radiation pattern of a directional antenna.



We then to calculate the antenna gain of the main lobe of a directional antenna and the antenna gain of the side-lobes and back-lobes, which are denoted as g_m and g_s , respectively. We first derive the maximum beamwidth θ_{max} of the main beam. As shown in Figure 10, we consider a sphere with radius r_d , where the radiated power of the main beam is concentrated within the small surface with area A . The area A can be approximated as $A = r_d \tan \theta_{max}/2$. We denote S as the surface area of the sphere. By Equation (3), we have

$$g_m = \frac{\frac{P_{rad}}{A}}{\frac{P_{rad}}{S}} = \frac{\frac{P_{rad}}{\pi r_d^2 \tan^2 \frac{\theta_{max}}{2}}}{\frac{P_{rad}}{4\pi r_d^2}} = \frac{4}{\tan^2 \frac{\theta_{max}}{2}} \tag{4}$$

We next derive the maximum approximated beamwidth θ_{max} for g_m .

$$\theta_{max} = 2 \arctan \sqrt{\frac{4}{g_m}} \tag{5}$$

Usually, the main beamwidth $\theta_m < \theta_{max}$. Similar to [15], we simply choose θ_m to be the largest multiple of 10 that is less than θ_{max} . Given θ_m and g_m , we now derive the antenna gain of side-lobes and back-lobes g_s as the following steps.

By Equation (3), we have

$$g_m \cdot \frac{P_{rad}}{S} \cdot A + g_s \cdot \frac{P_{rad}}{S} (S - A) = \eta \cdot P_{rad} \tag{6}$$

Solving the equation, we have

$$g_s = \frac{\eta \cdot \frac{S}{A} - g_m}{\frac{S}{A} - 1} \tag{7}$$

where $\frac{S}{A} = \frac{4}{\tan^2 \frac{\theta_{max}}{2}}$ and η is usually set to be 1.

We then calculate the main beam gain g_m by Equation (4). We next choose θ_m to be the largest multiple of 10 that is less than θ_{max} . Finally, we calculate the side-lobe and back-lobe gains by Equation (7). Table 2 lists both the linear gains and logarithmic gains (dBi).

Table 2. Antenna gains (linear and logarithmic).

Main Beamwidth θ_m	Main Beam Gain g_m	Side-Lobe and Back-Lobe Gain g_s
60°	10 (10 dBi)	0.18 (−7.4 dBi)
40°	25.12 (14 dBi)	0.17 (−7.6 dBi)
20°	100 (20 dBi)	0.22 (−6.5 dBi)
10°	398 (26 dBi)	0.398 (−4.0 dBi)

As shown in Table 2, when the main beamwidth of a directional antenna is decreased, the ratio of g_m/g_s is significantly increased. In particular, when the main beamwidth is quite narrow (e.g., $\theta_m \leq 10^\circ$), we have $g_m \gg g_s$.

6.2. Physical Channel Model

We denote the node whose transmission causes the interference to other nodes as the *interfering* node. The node whose reception is interfered by other *interfering* nodes is denoted as *interfered* node.

We assume that the interfering node transmits with power P_t . The received power at the interfered node at a distance d from the interfering node is denoted by P_r , which can be calculated by

$$P_r = CG_tG_rP_t \frac{1}{r^\alpha} \tag{8}$$

where C is a constant, G_t and G_r denote the antenna gain of the interfering node and the antenna gain of the interfered node, respectively, and α is the path loss factor usually ranging from 3 to 4 [28].

When an interfering node interferes with an interfered node, the received power at the interfered node P_r is required to be no less than a threshold P_0 , i.e., $P_r \geq P_0$. Thus, to calculate P_0 , we

$$P_0 = CG_tG_rP_t \frac{1}{R_i^\alpha} \tag{9}$$

where R_i is defined as the *interfering range* in the physical channel model.

Solving this equation, we have

$$R_i = \left(\frac{CG_t G_r P_t}{P_0} \right)^{\frac{1}{\alpha}} \tag{10}$$

We next analyze the interfering range R_i according to the four different scenarios, which are summarized in Table 3.

Table 3. Four scenarios.

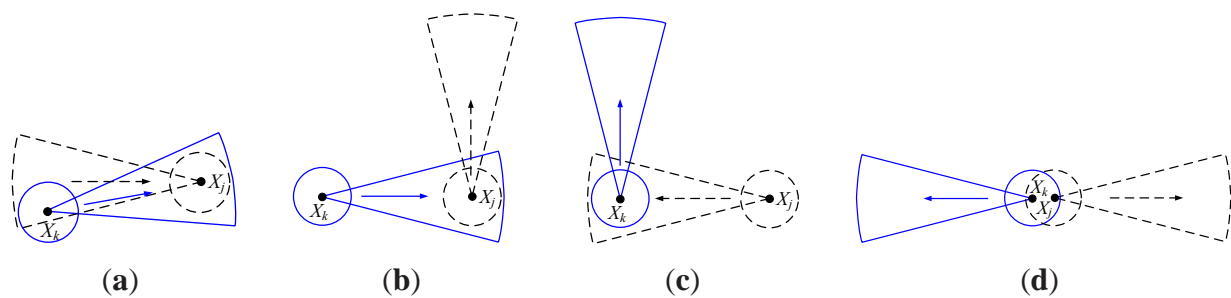
Scenarios	Interfering Node	Interfered Node	Interference Range R_i
I	Main beam	Main beam	$R_i(MM)$
II	Main beam	Side-lobes and back-lobes	$R_i(MS)$
III	Side-lobes and back-lobes	Main beam	$R_i(SM)$
IV	Side-lobes and back-lobes	Side-lobes and back-lobes	$R_i(SS)$

In particular, in Scenario I, two nodes X_j and X_k interfere with each other if and only if they fall into the interference range of each other and their main antenna beams are pointed toward each other, as shown in Figure 11(a). In this case, the interference range denoted by $R_i(MM)$ can be calculated by

$$R_i(MM) = \left(\frac{Cg_m g_m P_t}{P_0} \right)^{\frac{1}{\alpha}} \tag{11}$$

where we replace both G_t and G_r in Equation (10) by g_m .

Figure 11. Four scenarios. (a) Scenario (I); (b) Scenario (II); (c) Scenario (III); (d) Scenario (IV).



In Scenario II, the main antenna beam of the interfering node X_k is pointed to the interfered node X_j , which also falls into the interference range of X_i . However, the main beam of the interfered node X_j is not necessarily pointed to the interfering node X_k . Due to the existence of the side-lobes and the back-lobes, the reception of node X_j is interfered by node X_k , as shown Figure 11(b). Thus, the interference range denoted by $R_i(MS)$ can be calculated by

$$R_i(MS) = \left(\frac{Cg_m g_s P_t}{P_0} \right)^{\frac{1}{\alpha}} \tag{12}$$

where we replace G_t and G_r in Equation (10) by g_m and g_s , respectively.

Similar to Scenario II, the interference range in Scenario III, which is denoted by $R_i(MS)$, can be calculated by

$$R_i(SM) = \left(\frac{Cg_s g_m P_t}{P_0}\right)^{\frac{1}{\alpha}} \tag{13}$$

where we replace G_t and G_r in Equation (10) by g_s and g_m , respectively.

It is obvious that $R_i(MS) = R_i(SM)$. Thus, we regard $R_i(MS)$ as $R_i(SM)$ interchangeably throughout the remaining paper.

In Scenario IV, the side-/back-lobes of the interfering node X_k and the interfered node X_j cover each other. Thus, we can calculate the interference range denoted by $R_i(SS)$

$$R_i(SS) = \left(\frac{Cg_s g_s P_t}{P_0}\right)^{\frac{1}{\alpha}} \tag{14}$$

where we replace both G_t and G_r in Equation (10) by g_s .

With regard to $R_i(SS)$, $R_i(MS)$ and $R_i(MM)$, we have the following result, which can be used to compare the different interference ranges under the above scenarios.

Lemma 3 *When the main beamwidth θ_m is narrow, we have $R_i(SS) \ll R_i(MS) \ll R_i(MM)$.*

Proof. First, we have

$$\frac{R_i(SS)}{R_i(MS)} = \frac{\left(\frac{Cg_s g_s P_t}{P_0}\right)^{\frac{1}{\alpha}}}{\left(\frac{Cg_m g_s P_t}{P_0}\right)^{\frac{1}{\alpha}}} = \left(\frac{g_s}{g_m}\right)^{\frac{1}{\alpha}} \tag{15}$$

Similarly, we have

$$\frac{R_i(MS)}{R_i(MM)} = \left(\frac{g_s}{g_m}\right)^{\frac{1}{\alpha}} \tag{16}$$

As shown in Table 2, when the beamwidth θ_m is narrow (e.g., $\theta_m \leq 10^\circ$), $g_s \ll g_m$. Since the path loss factor α usually ranges from 2 to 4, it is obvious that $R_i(SS) \ll R_i(MS) \ll R_i(MM)$. \square

We then follow the similar steps in Theorem 1 and derive the upper bounds on the number of channels with consideration of side-lobes and back-lobes.

Theorem 8 *If there are n nodes in a planar area with the density D and each node is equipped with a directional antenna with the beamwidth θ_m , the main beam gain g_m and the side-/back-lobes gain g_s , for any valid link set LS derived from the n nodes, the corresponding conflict graph $G(LS)$ can be colored by using $2D + \frac{4\pi D}{\theta_m} \cdot \left(\frac{g_s}{g_m}\right)^{\frac{2}{\alpha}} - 1$ colors.*

Proof. Consider link l_{ij} that consists of two nodes X_i and X_j . The distance between X_i and X_j is denoted by d . To ensure that X_i can communicate with X_j , we require $d \leq R_t$, where R_t is the transmission range of X_i . The area of the interference region (including the interference region of the main beam as well as the interference region of the side-/back-lobes) varies with the different distance d . However, d cannot be too large, otherwise X_i and X_j cannot communicate with each other. It holds that $d \leq R_t$. To simply our analysis, we consider the following two cases.

Case 1 (when $d = R_t$):

In this case, the interference region of side-/back-lobes is totally covered by the interference region of the main beam of a directional antenna as shown in Figure 12(a). This is because the interference range

of side-/back-lobes denoted by $R_i(SS)$ or $R_i(MS)$ (note it depends on whether the interfering node is pointing its main beam or its side-/back-lobes toward the interfered node) is far less than the interference range of the main beam denoted by $R_i(MM)$ as proved in Lemma 3.

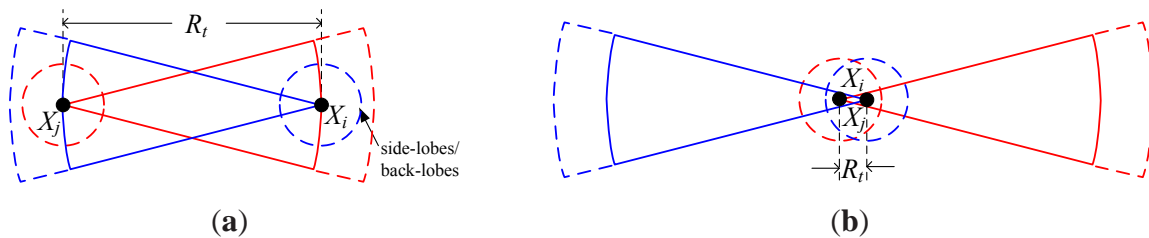
Following the proof of Theorem 1, the interference region contains no more than $2D - 2$ nodes excluding nodes X_i and X_j . From Lemma 1, the conflict graph can be colored by $2D - 1$ colors.

Case 2 (when $d < R_i$):

When the distance d is decreased, the interference region caused by the side-/back-lobes may not be totally covered by the interference region of the main beam. For example, there is an extreme case (when $d \rightarrow 0$), as shown in Figure 12(b), where the interference region consists of two sectors of main lobes and two circles of side-/back lobes, which cannot be totally covered by the interference region of the main lobes. In this case, the interference region has the maximum coverage area.

We then calculate the number of nodes in this interference region. The number of nodes in the two circles is at most $\frac{D}{\frac{\theta_m}{2}(R_i(MM))^2} \cdot 2\pi(R_i(MS))^2 = \frac{4\pi D}{\theta_m} \cdot (\frac{g_s}{g_m})^{\frac{2}{\alpha}}$, which is obtained by Equation (16) of Lemma 3. Note that we choose $R_i(MS)$ instead of $R_i(SS)$ because $R_i(MS) \gg R_i(SS)$. Besides, the number of nodes in the two sectors is at most $2D - 2$. Thus, there are at most $2D - 2 + \frac{4\pi D}{\theta_m} \cdot (\frac{g_s}{g_m})^{\frac{2}{\alpha}}$ nodes in the interference region. From Lemma 1, the conflict graph can be colored by $2D + \frac{2\pi D}{\theta_m} \cdot (\frac{g_s}{g_m})^{\frac{2}{\alpha}} - 1$ colors. □

Figure 12. Two cases for Theorem 8. (a) Case 1; (b) Case 2.



As shown in Theorem 8, the upper bound on the number of channels is $2D + \frac{2\pi D}{\theta_m} \cdot (\frac{g_s}{g_m})^{\frac{2}{\alpha}} - 1$. When the beamwidth θ_m of a directional antenna is narrow, the term $\frac{2\pi D}{\theta_m} \cdot (\frac{g_s}{g_m})^{\frac{2}{\alpha}}$ is so small that we can often ignore the effect of the side-/back-lobes.

7. Conclusions

Many previous studies are focused on using multiple channels in wireless networks with omni-directional antennas, which have high interference. There are few studies considering multiple channels in wireless networks with directional antennas, which can lead to low interference. In this paper, we study the channel allocation problem in wireless networks with directional antennas. In particular, we derive the upper bounds on the number of channels to ensure the collision-free communication in multi-channel wireless networks using directional antennas. We found that the upper bounds heavily depend on the node density and are also related to the interference ratio. Our results can be used to estimate the number of channels in practical wireless networks.

Acknowledgements

The work described in this paper was supported by Macao Science and Technology Development Fund under Grant No. 036/2011/A. The authors would like to thank Guodong Han for his valuable comments.

References

1. Zhang, J.; Jia, X.; Zhou, Y. Analysis of capacity improvement by directional antennas in wireless sensor networks. *ACM Trans. Sensor Netw.* **2012**, *9*, 1–3.
2. Dai, H.N. Throughput and Delay in Wireless Sensor Networks Using Directional Antennas. In Proceedings of the Fifth International Conference on Intelligent Sensors, Sensor Networks and Information Processing (ISSNIP), Melbourne, Australia, 7–10 December 2009.
3. Raniwala, A.; Chiueh, T. Architecture and Algorithms for an IEEE 802.11-Based Multi-Channel Wireless Mesh Network. In Proceedings of International Conference on Computer Communications (INFOCOM), Miami, FL, USA, 13–17 March 2005.
4. So, J.; Vaidya, N.H. Multi-Channel MAC for *Ad Hoc* Networks: Handling Multi-Channel Hidden Terminals Using a Single Transceiver. In Proceedings of ACM International Symposium on Mobile *Ad Hoc* Networking and Computing (MobiHoc), Tokyo, Japan, 24–26 May 2004.
5. Kyasanur, P.; Vaidya, N.H. Routing and Interface Assignment in Multi-Channel Multi-Interface Wireless Networks. In Proceedings of IEEE Wireless Communications and Networking Conference (WCNC), New Orleans, LA, USA, 13–17 March 2005.
6. Nasipuri, A.; Zhuang, J.; Das, S. A Multichannel CSMA MAC Protocol for Multihop Wireless Networks. In Proceedings of IEEE Wireless Communications and Networking Conference (WCNC), New Orleans, LA, USA, 21–24 September 1999.
7. Bahl, P.; Chandra, R.; Dunagan, J. SSCH: Slotted Seeded Channel Hopping for Capacity Improvement in IEEE 802.11 Ad-Hoc Wireless Networks. In Proceedings of ACM International Conference on Mobile Computing and Networking (MobiCom), Philadelphia, PA, USA, 26 September–1 October 2004.
8. Draves, R.; Padhye, J.; Zill, B. Routing in Multi-Radio, Multi-Hop Wireless Mesh Networks. In Proceedings of ACM International Conference on Mobile Computing and Networking (MobiCom), Philadelphia, PA, USA, 26 September–1 October 2004.
9. Kyasanur, P.; Vaidya, N.H. Capacity of MultiChannel Wireless Networks: Impact of Number of Channels and Interfaces. In Proceedings of ACM International Conference on Mobile Computing and Networking (MobiCom), Cologne, Germany, 28 August–2 September 2005.
10. S Kodialam, M.; Nandagopal, T. Characterizing the Capacity Region in Multi-Radio Multi-Channel Wireless Mesh Networks. In Proceedings of ACM International Conference on Mobile Computing and Networking (MobiCom), Cologne, Germany, 28 August–2 September 2005.
11. Jain, K.; Padhye, J.; Padmanabhan, V.N.; Qiu, L. Impact of Interference on Multi-Hop Wireless Network Performance. In Proceedings of ACM International Conference on Mobile Computing and Networking (MobiCom), San Diego, CA, USA, 14–19 September 2003.

12. Cao, L.; Wu, M.Y. Upper Bound of the Number of Channels for Conflict-free Communication in Multi-Channel Wireless Networks. In Proceedings of IEEE Wireless Communications and Networking Conference (WCNC), Hong Kong, China, 11–15 March 2007.
13. Li, W.W.L.; Zhang, Y.J.; So, A.M.C.; Win, M.Z. Slow adaptive OFDMA systems through chance constrained programming. *IEEE Trans. Signal Process.* **2010**, *58*, 3858–3869.
14. Yi, S.; Pei, Y.; Kalyanaraman, S. On the Capacity Improvement of *Ad Hoc* Wireless Networks Using Directional Antennas. In Proceedings of ACM International Symposium on Mobile *Ad Hoc* Networking and Computing (MobiHoc), Annapolis, MD, USA, 1–3 June 2003.
15. Ramanathan, R. On the Performance of *Ad Hoc* Networks with Beamforming Antennas. In Proceedings of ACM International Symposium on Mobile *Ad Hoc* Networking and Computing (MobiHoc), Long Beach, CA, USA, 4–5 October 2001.
16. Takai, M.; Martin, J.; Bagrodia, R.; Ren, A. Directional Virtual Carrier Sensing for Directional Antennas in Mobile *Ad Hoc* Networks. In Proceedings of ACM International Symposium on Mobile *Ad Hoc* Networking and Computing (MobiHoc), Lausanne, Switzerland, 9–11 June 2002.
17. Choudhury, R.R.; Yang, X.; Vaidya, N.H.; Ramanathan, R. Using Directional Antennas for Medium Access Control in *Ad Hoc* Networks. In Proceedings of ACM International Conference on Mobile Computing and Networking (MobiCom), Atlanta, GA, USA, 23–28 September 2002.
18. Korakis, T.; Jakllari, G.; Tassiulas, L. A MAC Protocol for Full Exploitation of Directional Antennas in Ad-Hoc Wireless Networks. In Proceedings of ACM International Symposium on Mobile *Ad Hoc* Networking and Computing (MobiHoc), Annapolis, MD, USA, 1–3 June 2003.
19. Zhang, Z. Pure Directional Transmission and Reception Algorithms in Wireless *Ad Hoc* Networks with Directional Antennas. In Proceedings of IEEE International Conference on Communications, Seoul, Korea, 16–20 May 2005.
20. Ramanathan, R.; Redi, J.; Santivanez, C.; Wiggins, D.; Polit, S. *Ad Hoc* Networking with Directional Antennas: A Complete System Solution. *IEEE JSAC* **2005**, *23*, 496–506.
21. Dai, H.N.; Ng, K.W.; Wu, M.Y. A Busy-Tone based MAC Scheme for Wireless *Ad Hoc* Networks Using Directional Antennas. In Proceedings of IEEE Globecom, Washington, DC, USA, 26–30 November 2007.
22. Dai, H.N.; Ng, K.W.; Wong, R.C.W.; Wu, M.Y. On the Capacity of Multi-Channel Wireless Networks Using Directional Antennas. In Proceedings of International Conference on Computer Communications (INFOCOM), Phoenix, AZ, USA, 13–18 April 2008.
23. Raman, B. Channel Allocation in 802.11-Based Mesh Networks. In Proceedings of International Conference on Computer Communications (INFOCOM), Barcelona, Spain, 23–29 April 2006.
24. Gupta, P.; Kumar, P.R. The capacity of wireless networks. *IEEE Trans. Inf. Theory* **2000**, *46*, 388–404.
25. West, D.B. *Introduction to Graph Theory*, 2nd ed.; Prentice Hall PTR: Upper Saddle River, NJ, USA, 2001.
26. Panconesi, A.; Rizzi, R. Some simple distributed algorithms for sparse networks. *Distrib. Comput.* **2001**, *14*, 97–100.
27. Szekeres, G.; Wilf, H.S. An inequality for the chromatic number of a graph. *J. Comb. Theory* **1968**, *4*, 1–3.

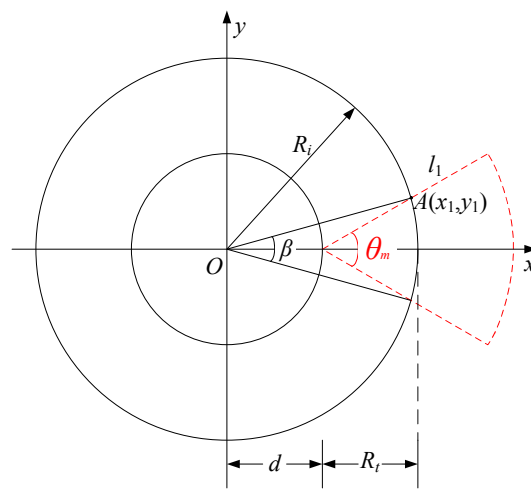
28. Rappaport, T.S. *Wireless Communications: Principles and Practice*, 2nd ed.; Prentice Hall PTR: Upper Saddle River, NJ, USA, 2002.

A. Appendix 1. Calculation of the Coverage Angle β

To calculate the coverage angle β , we need to obtain coordinates x_1 and y_1 of the intersection point A first, as shown in Figure A1. The circle is denoted by the equation

$$x^2 + y^2 = R_i^2 \tag{17}$$

Figure A1. Calculate the coverage angle β .



The line l_1 is denoted by the equation

$$y = \tan \frac{\theta_m}{2} \cdot (x - d) \tag{18}$$

After joining Equations (17) and (18), we have the coordinates x and y of the point A .

$$x_1 = \frac{d \cdot \tan^2 \frac{\theta_m}{2} + \sqrt{(R_i^2 - d^2) \tan^2 \frac{\theta_m}{2} + R_i^2}}{1 + \tan^2 \frac{\theta_m}{2}} \tag{19}$$

$$y_1 = \tan \frac{\theta_m}{2} \cdot \frac{\sqrt{(R_i^2 - d^2) \tan^2 \frac{\theta_m}{2} + R_i^2} - d}{1 + \tan^2 \frac{\theta_m}{2}} \tag{20}$$

On the other hand, we have $\tan \frac{\beta}{2} = \frac{y_1}{x_1} = \frac{\tan \frac{\theta_m}{2} \cdot (\sqrt{(R_i^2 - d^2) \tan^2 \frac{\theta_m}{2} + R_i^2} - d)}{d \tan^2 \frac{\theta_m}{2} + \sqrt{(R_i^2 - d^2) \tan^2 \frac{\theta_m}{2} + R_i^2}}$. Thus, we have

$$\beta = 2 \arctan \left(\frac{\tan \frac{\theta_m}{2} \cdot (\sqrt{(R_i^2 - d^2) \tan^2 \frac{\theta_m}{2} + R_i^2} - d)}{d \tan^2 \frac{\theta_m}{2} + \sqrt{(R_i^2 - d^2) \tan^2 \frac{\theta_m}{2} + R_i^2}} \right) \tag{21}$$

□